ACTA IMEKO
ISSN: 2221-870X
December 2023, Volume 12, Number 4, 1 - 6

Comparison of volume and centroid uncertainty of a cylindrical segment by two different methods

Ronan Alves da Paixão[1], André Melo Carvalhais Dutra[2], Elcio Cruz de Oliveira[1,3]

[1] *Postgraduate Programme in Metrology, Pontifical Catholic University of Rio de Janeiro, R. Marquês de São Vicente 225, 22451-900 Rio de Janeiro, Brazil*
[2] *CTR3SM Tecnologias Críticas, Av. Raja Gabaglia, 2000, Sala 232 Pavmto 2 Bloco 1, 30494-170, Belo Horizonte, Brazil*
[3] *Logistics, Operational Planning and Control, Measurement and Product Inventory Management, PETROBRAS S.A., Av. Henrique Valadares28, 20231-030 Rio de Janeiro, Brazil*

ABSTRACT
The cylindrical segments, which have applications in novel tilt-based industrial hydrometers, are seldom studied analytically, unlike spheres, cylinders, and parallelepipeds. More specifically, the cylindrical segment has two means of being characterized: by measuring the radius, the middle height, and the cutting angle; and by measuring the radius and both the minimum and the maximum heights. In other words, the literature presents two different sets of algorithms for calculating the characteristics of the cylindrical segment. This study sheds light on one equation from the literature about the cylindrical segment that must be corrected. Next, the two measurement forms are compared, along with their impact on the uncertainty of the volume and barycenter of this solid. Routine applications depend on specific input uncertainties, measurements, and objectives. Still, for most cases, it turned out that measuring the minimum and maximum heights generally provides lower uncertainty values for the evaluated calculations instead of measuring the height of the cylinder's axis and the angle, especially the centroids.

Section: RESEARCH PAPER

Keywords: Volume and centroid uncertainty; cylindrical segment; solid barycenter parallelepipeds

Citation: Ronan Alves da Paixão, André Melo Carvalhais Dutra, Elcio Cruz de Oliveira, Comparison of volume and centroid uncertainty of a cylindrical segment by two different methods,Acta IMEKO, vol. 12, no. 4, article 5, December 2023, identifier: IMEKO-ACTA-12 (2023)-04-05

Section Editor: Eric Benoit, Université Savoie Mont Blanc, France

Received June 28, 2022; **In final form** September 11, 2023; **Published** December2023

Funding: The author thanks Coordenação de Aperfeiçoamento de Pessoal de Nível Superior (CAPES, Brazil) Finance code 001 and the scholarship from the Brazilian agency CNPq (305479/2021-0).

Corresponding author: Elcio Cruz de Oliveira, e-mail: elciooliveira@puc-rio.br

1. INTRODUCTION

Even though industrial processes are increasing the usage of automation technology, the application of uncertainty methods is not so predominant as a quality parameter [1]-[3]. Despite its low industrial usage, measurement uncertainty estimation can be considered as a critical metrological assessment tool of the measurement system [4], [5].

Although type A evaluation results – uncertainty assessment method by statistical analysis of a series of observations, such as experimental standard deviation – are easier to obtain by comparing the results of an instrument with a reference, it is not always straightforward, considering that the algebraic relationships needed to plot some uncertainty chains are not always available. In addition, sometimes it is impractical to quantify some kinds of type B assessments, i.e., previous measurement data, expertise of the operator in that activity, specifications of manufacturer and data provided in calibration certificates and datasheets [6]. This realization makes some instrument designers rely on experimentally fitted curves rather than analytical models. However, the uncertainty derived from algebraic formulas can offer good insights into what can be done to improve the construction of a device.

This is the case of artisanal beer brewing, where an experiment can take anywhere from a few hours to a few weeks [7] and several variables are involved. In this case, there is an instrument that significantly reduces manual quality control, eliminating many sources of uncertainty which would be evaluated as type B. To build the formulas associated with this instrument, it was necessary to investigate the uncertainty of its volume, which involves the analysis of a cylindrical segment.

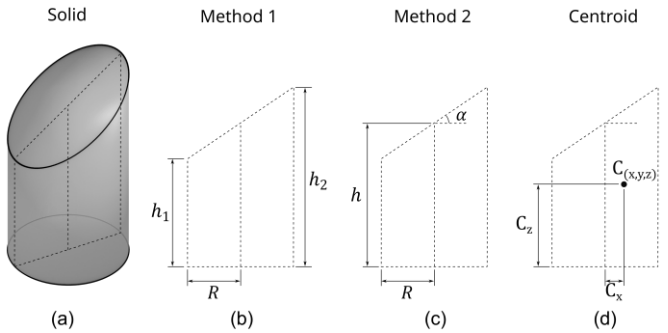

Figure 1. A cylindrical segment (a), which are usually represented by two sets of variables – (b) and (c) – that can be measured by two different methods, and a graphical representation of the centroid (d). (b), (c) and (d) are representations of the cylindrical segment's cross-section through its cut's major axis.

While it can be easy to find the characteristics of commonly used solids like spheres, cylinders and parallelepipeds, others are not so easy to discover. One of those is the cylindrical segment. Additionally, the characteristics of the cylindrical segment can be calculated by two different methods: Method 1, measurement of the radius and length of the biggest and shortest heights, and Method 2, measurement of the radius, the height of the cylinder's axis, and the cutting plane angle (Figure 1). In Figure 1, h is the height of the cylinder's axis; h_1 is the minimum height of the cylinder segment; h_2 is the maximum height of the cylinder segment; R is the radius of the cylinder; α is the angle from the cutting plane to the bottommost circular cross-section; $C_{(x,y,z)}$ is the graphical representation of the cylinder's centroid, C_x is its horizontal distance from the axis of the cylinder, C_y is always zero (the cylinder cut is considered perpendicular to the Y plane) and C_z is its vertical distance from the bottom of the cylinder. In this work, the measurement of the radius was considered to have the same characteristics of the measurement of the diameter.

If one can select from multiple measurement instruments, not only of different uncertainties but also of different quantities or even natures, there can be multiple ways of determining the uncertainty of the measurand based on different mathematical models. In the case of the volume and centroid of a cylindrical segment, which has at least two measurement methods, the best match can be found by applying the uncertainties of reference instruments and estimating the uncertainties of the target properties from their formulas and calculating the results by applying the Guide to the expression of uncertainty in measurement (GUM) technique [8].

The aim of this study is to compare those two measurement methods. The first step is to enumerate some equations that might be of interest and shed light to a researcher on the properties of tilt hydrometers [9]-[11]. Practical recent studies that use this principle can be applied in diverse scientific applications such as a small multi-rotor airship [12], a hydrodynamic model of robots [13], a glider [14], geometrical parameters of the hull ship [15]-[17], a stratospheric airship [18], swimsuits [19], [20] and artisanal and small-scale beer brewing instruments [21]. The second step is to estimate the uncertainties associated with each measurand and calculate their impact on the combined uncertainties of those equations. Lastly, some comments are made about how a researcher might choose which method better fits a specific purpose, depending on the application's needs, the measurement instruments' uncertainties and the importance given for each variable.

2. METHODOLOGY

2.1. The correct centroid

While the volume of a cylindrical segment may be found intuitively, the position of its barycenter is not calculated trivially. In the literature, two different equations are available for calculating the z coordinate of the barycenter, C_z [22], [23], respectively, Equation (1) and Equation (2):

$$C_z = \frac{h}{2} + \frac{R^2 \tan^2 \alpha}{2\,h} \tag{1}$$

$$C_z = \frac{h}{2} + \frac{R^2 \tan^2 \alpha}{8\,h}. \tag{2}$$

As Equations (1) and (2) are different by a single factor, one suspects that one of them is not correct. Let's consider that Equations (3) and (4) are available to convert from Method 1 to and from Method 2.

$$h = \frac{h_1 + h_2}{2} \tag{3}$$

$$\tan \alpha = \frac{h_2 - h_1}{2\,R}. \tag{4}$$

Thus, it is possible to substitute them in Equation (1) to contrast it with Equation (2), which yields Equation (5):

$$C_z = \frac{h_1 + h_2}{4} + \frac{R^2 \left(\frac{h_2 - h_1}{2\,R}\right)^2}{h_1 + h_2} = \frac{h_1^2 + h_2^2}{2\,(h_1 + h_2)}. \tag{5}$$

This is a different result from the one obtained by Weisstein [23], Equation (6):

$$C_z = \frac{5\,h_1^2 + 6\,h_1\,h_2 + 5\,h_2^2}{16\,(h_1 + h_2)} = \frac{h}{2} + \frac{R^2 \tan^2 \alpha}{8\,h}. \tag{6}$$

Therefore, the previous suspicion is confirmed. However, to ascertain which formula is correct, Equation (1) or Equation (6), it was preferable to calculate the center of mass by integrating the moments and dividing by the volume, considering that the barycenter is equal to the centroid in a solid with uniform density, Equation (7):

$$\frac{\int\int\int \vec{z}\, r\, \mathrm{d}z\, \mathrm{d}\theta\, \mathrm{d}r}{\pi\, R^2\, h} = \frac{\int_0^R \int_0^{2\,\pi} \int_0^{h(r,\,\alpha)} z\, r\, \mathrm{d}z\, \mathrm{d}\theta\, \mathrm{d}r}{\pi\, R^2 \left(\frac{h_1 + h_2}{2}\right)} \tag{7}$$

where $h(r, \alpha) = h_1 + \frac{1}{2}\left(1 + \frac{r}{R}\cos\alpha\right)(h_2 - h_1)$.

This results in the same formula of Weisstein [23], which settles the dispute, i.e., Equation (6) is the correct form. All other mathematical formulas are the same for the two methods after converting the variables.

2.2. Uncertainty evaluation

The formulas from Weisstein [23] can be expressed in two forms, Table 1. Conversion between the two forms can be made by using Equation (3) and Equation (4).

Here, it was considered that all variables are uncorrelated. On the other hand, if the nonlinearities that arise from the angular equations become a source of concern, the researcher can also investigate higher-order Taylor series expansions or Monte Carlo methods [24], [25]. Cylindricity errors [1] are considered out of scope for this study.

Table 1. Formulas for cylindrical segment properties.

Quantities	Method 1: R, h_1, h_2	Method 2: R, h, α
Volume	$\pi R^2 \left(\frac{h_1+h_2}{2}\right)$	$\pi R^2 h$
Centroid for x	$\frac{R(h_2-h_1)}{4(h_1+h_2)}$	$\frac{R^2 \tan\alpha}{4h}$
Centroid for y	0	0
Centroid for z	$\frac{5h_1^2+6h_1h_2+5h_2^2}{16(h_1+h_2)}$	$\frac{h}{2}+\frac{R^2\tan^2\alpha}{8h}$

2.3. Comparing the approaches

Starting with the volume, calculating the two different equations for volume in Table 1 yields:

Method 1: $V_1 = f(R,h_1,h_2) = \frac{\pi R^2 (h_1+h_2)}{2}$

The relative combined uncertainty is expressed in Equation (8):

$$\begin{aligned}\frac{u_{c_1}^2(V_1)}{V_1^2} &= \left(\frac{\partial f}{\partial R}\right)^2 \frac{u_1^2(R)}{V_1^2} + \left(\frac{\partial f}{\partial h_1}\right)^2 \frac{u_1^2(h_1)}{V_1^2} \\ &\quad + \left(\frac{\partial f}{\partial h_2}\right)^2 \frac{u_1^2(h_2)}{V_1^2} \\ \frac{u_{c_1}^2(V_1)}{V_1^2} &= \frac{4}{R^2}u_1^2(R) + \frac{1}{(h_1+h_2)^2}u_1^2(h_1) \\ &\quad + \frac{1}{(h_1+h_2)^2}u_1^2(h_2)\,.\end{aligned} \tag{8}$$

Method 2: $V_2 = f(R,h) = \pi R^2 h$

The relative combined uncertainty is expressed in Equation (9):

$$\begin{aligned}\frac{u_{c_2}^2(V_2)}{V_2^2} &= \left(\frac{\partial f}{\partial R}\right)^2 \frac{u_2^2(R)}{V_2^2} + \left(\frac{\partial f}{\partial h}\right)^2 \frac{u_2^2(h)}{V_2^2} \\ &= \frac{4}{R^2}u_2^2(R) + \frac{1}{h^2}u_2^2(h)\,.\end{aligned} \tag{9}$$

Related to the centroid for x, the exact same methods can be applied to both the x and z centroids.

Method 1: $C_{x1} = f(R,h_1,h_2) = \frac{R(h_2-h_1)}{4(h_1+h_2)}$

The relative combined uncertainty is expressed in Equation (10):

$$\begin{aligned}\frac{u_{c_1}^2(C_{x1})}{C_{x1}^2} &= \left(\frac{\partial f}{\partial R}\right)^2 \frac{u_1^2(R)}{C_x^2} + \left(\frac{\partial f}{\partial h_1}\right)^2 \frac{u_1^2(h_1)}{C_x^2} \\ &\quad + \left(\frac{\partial f}{\partial h_2}\right)^2 \frac{u_1^2(h_2)}{C_x^2} \\ &= \frac{1}{R^2}u_1^2(R) + \frac{4h_2^2}{(h_1-h_2)^2(h_1+h_2)^2}u_1^2(h_1) \\ &\quad + \frac{4h_1^2}{(h_1-h_2)^2(h_1+h_2)^2}u_1^2(h_2)\,.\end{aligned} \tag{10}$$

Method 2: $C_{x2} = f(R,h,\alpha) = \frac{R^2\tan(\alpha)}{4h}$

The relative combined uncertainty is expressed in Equation (11):

$$\begin{aligned}\frac{u_{c_2}^2(C_{x2})}{C_{x2}^2} &= \left(\frac{\partial f}{\partial R}\right)^2 \frac{u_2^2(R)}{C_x^2} + \left(\frac{\partial f}{\partial \alpha}\right)^2 \frac{u_2^2(\alpha)}{C_x^2} + \left(\frac{\partial f}{\partial h}\right)^2 \frac{u_2^2(h)}{C_x^2} \\ &= \frac{4}{R^2}u_2^2(R) + \frac{4}{\sin^2(2\alpha)}u_2^2(\alpha) + \frac{1}{h^2}u_2^2(h).\end{aligned} \tag{11}$$

When the same methodology is applied to the z centroid, it is much harder to read clearly.

Method 1: $C_{z1} = f(R,h_1,h_2) = \frac{5h_1^2+6h_1h_2+5h_2^2}{16h_1+16h_2}$

The relative combined uncertainty is expressed in Equation (12):

$$\begin{aligned}\frac{u_{c_1}^2(C_{z1})}{C_{z1}^2} &= \left(\frac{\partial f}{\partial h_1}\right)^2 \frac{u_1^2(h_1)}{C_z^2} + \left(\frac{\partial f}{\partial h_2}\right)^2 \frac{u_1^2(h_2)}{C_z^2} \\ &= \frac{(5h_1^2+10h_1h_2+h_2^2)^2}{(5h_1^3+11h_1^2h_2+11h_1h_2^2+5h_2^3)^2}u_1^2(h_1) \\ &\quad + \frac{(h_1^2+10h_1h_2+5h_2^2)^2}{(5h_1^3+11h_1^2h_2+11h_1h_2^2+5h_2^3)^2}u_1^2(h_2)\,.\end{aligned} \tag{12}$$

Method 2: $C_{z2} = f(R,h,\alpha) = \frac{R^2\tan^2(\alpha)}{8h} + \frac{h}{2}$

The relative combined uncertainty gets, Equation (13):

$$\begin{aligned}\frac{u_{c_2}^2(C_{z2})}{C_{z2}^2} &= \left(\frac{\partial f}{\partial R}\right)^2 \frac{u_2^2(R)}{C_z^2} + \left(\frac{\partial f}{\partial \alpha}\right)^2 \frac{u_2^2(\alpha)}{C_z^2} \\ &\quad + \left(\frac{\partial f}{\partial h}\right)^2 \frac{u_2^2(h)}{C_z^2} \\ &= \frac{4R^2\tan^4(\alpha)}{(R^2\tan^2(\alpha)+4h^2)^2}u_2^2(R) \\ &\quad + \frac{4R^4\tan^2(\alpha)}{(R^2\tan^2(\alpha)+4h^2)^2\cos^4(\alpha)}u_2^2(\alpha) \\ &\quad + \frac{\left(4h^2-R^2\tan^2(\alpha)\right)^2}{h^2(R^2\tan^2(\alpha)+4h^2)^2}u_2^2(h)\,.\end{aligned} \tag{13}$$

3. RESULTS AND DISCUSSION

In this section, the uncertainties are treated as a function of the independent variables for each equation and method. To be clearer when making comparisons, especially when using h_1 and h_2, the method number was applied as a subscript to the volume functions (V_1 and V_2) and their respective combined uncertainties (u_{c_1} and u_{c_2}).

3.1. Volume

To better make a comparison, the plot in Figure 2 was drawn. Empirical values of $R = 22.5$ mm, $h_1 = 61$ mm, $h_2 = 106$ mm, and $h = 83.5$ mm were used. Those references were chosen as they match the dimensions of another study the authors are working on, plus an initial supposition of a 45-degree angle. This angle was also chosen for analysis to minimize the

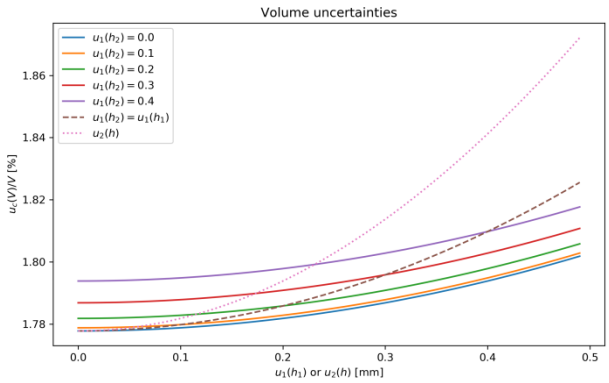

Figure 2. Uncertainties for volume. Solid lines are for Method 1 ($u_1(h_2)$), dashed line is for Method 1 with equal height uncertainties ($u_1(h_2) = u_1(h_1)$) and dotted line is for Method 2 ($u_2(h)$).

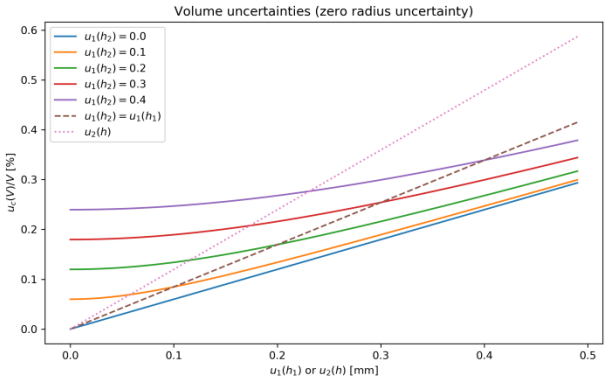

Figure 3. Volume uncertainties if radius uncertainty is equal to zero. Solid lines are for method 1, the dashed line is for method 1 with equal height uncertainties and the dotted line is for method 2.

effects of the nonlinearity brought by trigonometric functions, especially the tangent. The results and conclusions can vary depending on the magnitude of the actual quantity values.

A range of h_2 values was plotted for comparison. For Method 2, only a single line was drawn since it only has two variables. The value of $u_{1,2}(R) = 0.2$ mm was used for all calculations, except where noted (Figure 3) since the radius uncertainty is not affected by the height uncertainties. From Figure 2, it is interesting to note that Method 2 (dotted line) starts with a very small uncertainty result but increases rapidly when the uncertainty of the height measurement increases. Another surprising result was obtained by plotting a line where $u_1(h_1) = u_1(h_2)$ (dashed line). This equality is commonly encountered because these two linear measurements are usually taken by the same instrument. This contrasts with the dotted line, which increases faster. To mathematically investigate this behavior, it is possible to substitute those uncertainties with a single one, $u_1(h_{1,2})$, in Equation (8):

$$\begin{aligned}\frac{u_{c_1}^2(V_1)}{V_1^2} &= \frac{4}{R^2}u_1^2(R) + \frac{1}{(h_1+h_2)^2}u_1^2(h_1) \\ &+ \frac{1}{(h_1+h_2)^2}u_1^2(h_2) \\ &= \frac{4}{R^2}u_1^2(R) + \frac{2}{(h_1+h_2)^2}u_1^2(h_{1,2})\,.\end{aligned} \tag{14}$$

This contrasts with the result obtained by Method 2 on Equation (9), when replacing $h = \frac{h_1+h_2}{2}$:

$$\begin{aligned}\frac{u_{c_2}^2(V_2)}{V_2^2} &= \frac{4}{R^2}u_2^2(R) + \frac{1}{h^2}u_2^2(h) \\ &= \frac{4}{R^2}u_2^2(R) + \frac{4}{(h_1+h_2)^2}u_2^2(h)\end{aligned} \tag{15}$$

The results differ by a factor of 2 in the second addend of the relative combined variance (or $\sqrt{2}$ for the relative combined uncertainty, if the first addend is nullified by zeroing the radius uncertainty), which can be considered equivalent to the production of two measurements for h. This effect can be viewed better when producing a plot with a zeroed uncertainty for R, Figure 3.

3.2. Centroid for x

The results are available in Figure 4 and Figure 5, Methods 1 and 2, respectively. Since there is a third variable (α) in Method 2, it was necessary to divide the plots of the two methods. For comparison purposes, the same vertical axis was maintained.

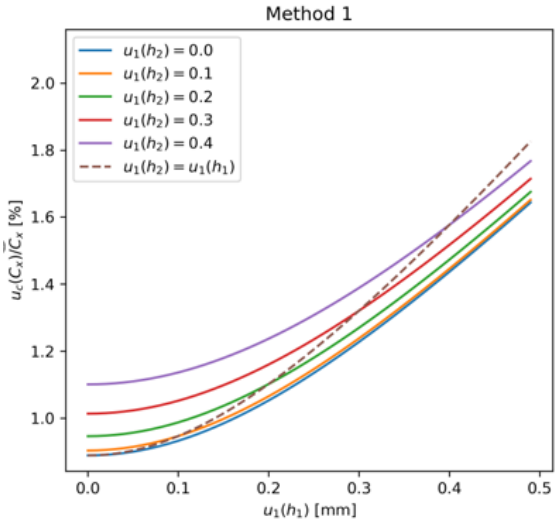

Figure 4. Uncertainties for the centroid in the X plane, Method 1.

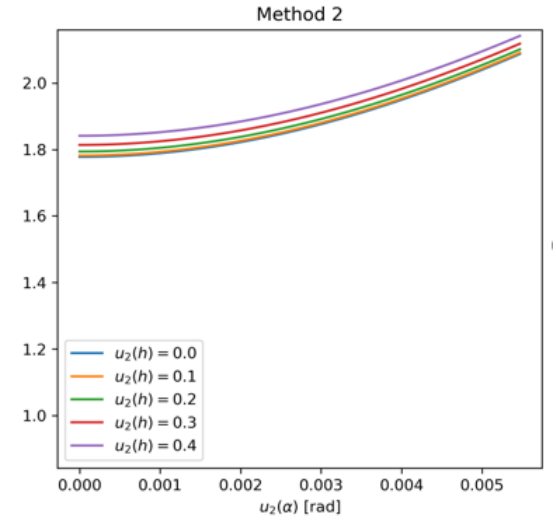

Figure 5. Uncertainties for the centroid in the X plane, Method 2.

For this case, however, it is harder to make comparisons since the uncertainty for Method 1 results in a function of two linear parameters (h_1 and h_2) and their uncertainties, while the uncertainty function for Method 2 presents one linear (h) and one angular (α) parameters and their uncertainties. Especially tricky is visualizing the role of a squared trigonometric function, $\sin^2(2\,\alpha)$ from Equation (11), in the final result. The horizontal scale of the plot for Method 2 was defined by taking the maximum uncertainty $u_1(h_1)$ from the plot for Method 1 (0.5 mm), making $u(h_2 - h_1) = u(h_2) + u(h_1) \approx 2\,u(h_1)$, adding that to $h_2 - h_1$, taking the arctangent of the angle created by the $2\,R$ and this line and then subtracting the original angle α (45° or $\pi/4$ radians) and using this value as the maximum uncertainty of α, or $u_2(\alpha)$. A schematic of the geometry calculations can be viewed in Figure 6.

Note that the lines for Method 2 are much closer together. This behavior indicates that the uncertainty is more affected by α than by h, since the same variation applied to $u_2(h)$ leads to a smaller variation in the combined uncertainty $u_c(C_x)$. Moreover, Method 1 appears to show smaller combined uncertainty for the chosen characteristics.

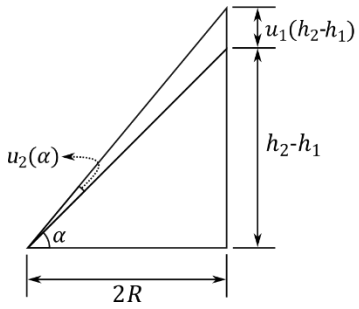

Figure 6. Schematic of the calculations done to obtain the maximum uncertainty for comparison of Method 2.

3.3. Centroid for z

It is interesting to note that, for method 1, R does not affect the uncertainty formula, i.e., R and $u(R)$ do not appear in Equation (12). This was expected since the uncertainties expressed here are relative, and the radius only proportionately affects the z centroid, Figure 7a, Figure 7b and Figure 7c.

The resulting subplot for method 2 (Figure 7b) appears very different from the others and presents almost horizontal lines. By investigating the behavior of the $u_2(h) = 0$ curve, which should be a straight line, it was suspected that the initial assumption for the range of $u_2(\alpha)$ was somewhat wrong for this case. Thus, another subplot was created, which increased the range of $u_2(\alpha)$ by an order of magnitude to allow for the observation of its effects over a longer span (Figure 7c).

In this case, it became very clear, from the increased distance between the lines for Method 2, that the effects of the uncertainty of $\boldsymbol{h}$ dominated over the effects of $\boldsymbol{\alpha}$ at the start of the $\boldsymbol{u(\alpha)}$ range, which prompted the change in presentation. By comparing Figure 7a, Figure 7b and Figure 7c, and assuming that the same measurement instrument is used for h_1, h_2 and h, which yields $u_1(h_1) = u_1(h_2) = u_1(h)$, one can see that the ratio between $u(h)$ and $u(\alpha)$ will determine the best method to use.

Practical applications should also consider that measuring the minimum and mean heights, respectively h_1 and h, is usually harder than measuring h_2 due to geometry and instrument constraints, e.g., a pachymeter does not lock to an oblique edge or to a specific point in a plane. This may increase $u_1(h_1)$ and $u_2(h)$.

Unfortunately, for the application currently in the study by the authors [8]-[10], Method 1 may not be available for practical purposes, which means that actual measurement uncertainties will have to rely on angle measurements. However, the comparison of these methods drew ideas that may be used in the future to build better sensors.

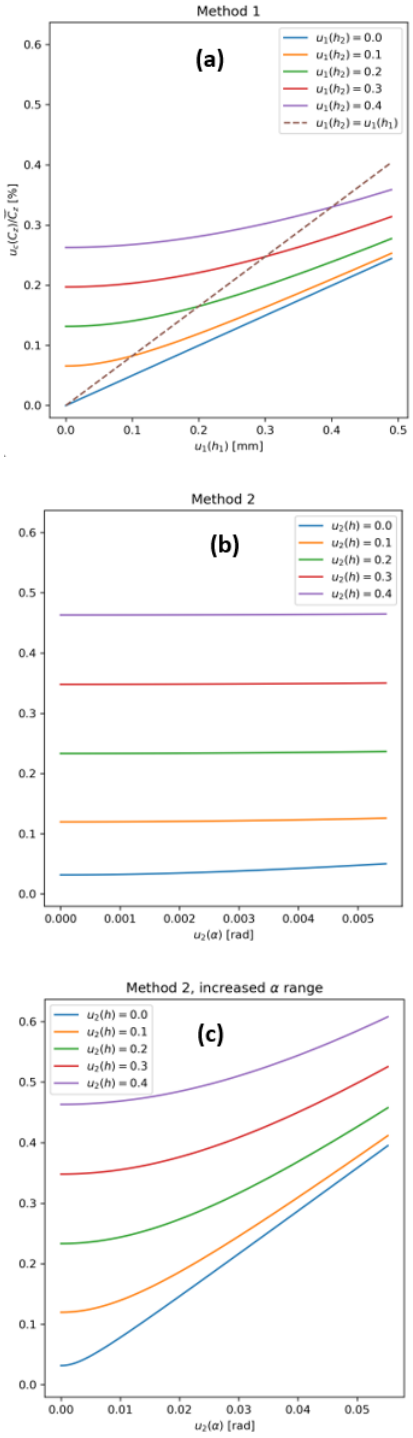

Figure 7. Uncertainties for the centroid in the Z plane. Subplot c) increases by ten times the $u_2(\alpha)$ range of subplot b).

4. CONCLUSIONS

From the comparison of the two methods, using the proper measurement method can improve the results. The careful weighting of the influence of every quantity on the uncertainty for each property can then help the researcher choose which method is more advantageous. In the case of the tilt hydrometer, the sensitivity of the final model to each of these uncertainties must be tested, if the method of measuring the two heights separately is possible.

While a definitive answer can only be found when comparing specific measurements, which vary with the problem to be solved, it appears that the method of measuring two heights is appropriate more often. Whereas the measurement of the minimum height h_1 is not easy, the difficulty of finding the true center of the cylinder segment to measure h must also be taken into consideration. Additionally, angle uncertainties are usually harder to reduce.

This work fills a gap in the analysis in the measurement of the cylindrical segment, which is a less common solid, but which can nonetheless be used in evaluating the measurement uncertainty of sensors.

ACKNOWLEDGEMENT

The authors thank for the financial support provided by the Brazilian funding agencies CNPq, CAPES, FINEP and FAPERJ. This study was financed in part by the Coordenação de Aperfeiçoamento de Pessoal de Nível Superior—Brasil (CAPES)—Finance Code 001.

REFERENCES

[1] A. Possolo, H. K. Iyer, Invited Article: Concepts and tools for the evaluation of measurement uncertainty. Review of Scientific Instruments, 88(1), 011301 (2017). DOI: 10.1063/1.4974274

[2] E. Heidaryan, A note on model selection based on the percentage of accuracy-precision. Journal of Energy Resources Technology, 141(4), 2019, 04550. DOI: 10.1115/1.4041844

[3] G. W. Forbes, M. A. Alonso, Measures of spread for periodic distributions and the associated uncertainty relations. American Journal of Physics, 69 (3) (2011), pp. 340 – 347. DOI: 10.1119/1.1317562

[4] E. C. de Oliveira, Critical metrological evaluation of fuel analyses by measurement uncertainty. Metrology and Measurement Systems, 18 (2), (2011), pp. 235–248. DOI: 10.2478/v10178-011-0006-4

[5] G. D'Emilia, A. Di Ilio, A. Gaspari, E. Natale, A. G. Stamopoulos, Uncertainty assessment for measurement and simulation in selective laser melting: A case study of an aerospace part. Acta IMEKO 9(2020) 4, pp. 96-105. DOI: 10.21014/acta_imeko.v9i4.720

[6] S. V. Gupta, Measurement Uncertainties: Physical Parameters and Calibration of Instruments, Springer Science & Business Media.

[7] C. White, J. Zainasheff, Yeast: The Practical Guide to Beer Fermentation (2010), Brewers Publications, Boulder, CO.

[8] JCGM100. (2008). Evaluation of measurement data — Guide to the expression of uncertainty in measurement, Published by the JCGM in the name of the BIPM, IEC, IFCC, ILAC, ISO, IUPAC, IUPAP, and OIML. Online [Accessed 9 June 2019] https://www.bipm.org/en/publications/guides/gum.html

[9] N. A. Baron, T. M. Bryant, Free Floating Tilt Hydrometer, US20140260607A1, 2014. Online [Accessed 6 November 2019] https://patents.google.com/patent/US20140260607/en

[10] N. A. Baron, T. M. Bryant, Free Floating Tilt Hydrometer, US9234828B2, 2016. Online [Accessed 6 November 2019] https://patents.google.com/patent/US9234828/en?oq=US+Patent+No.+9234828

[11] V. S. Lang, iSpindel - Die Idee, brau!magazin, 2018. Online [Accessed 22 April 2019] https://braumagazin.de/article/ispindel-die-idee/

[12] D. A. dos Santos, A. C. Junior, Flight control of a hexa-rotor airship: Uncertainty quantification for a range of temperature and pressure conditions. ISA Transactions, 93, (2019), pp. 268-279. DOI: 10.1016/j.isatra.2019.03.010

[13] Y. Li, F. Fish, Y. Chen, T. Ren, J. Zhou, Bio-inspired robotic dog paddling: kinematic and hydro-dynamic analysis, Bioinspir. Biomim. 14 (2019), 066008. DOI: 10.1088/1748-3190/ab3d05

[14] L. Gao, B. Li, L. Gao, Physical Modeling for the Gradual Change of Pitch Angle of Underwater Glider in Sea Trial, IEEE Journal of Oceanic Engineering (2018) 43, pp. 905-912. DOI: 10.1109/JOE.2017.2769918

[15] A. Nazemian, P. Ghadimi, Global optimization of trimaran hull form to get minimum resistance by slender body method, Journal of the Brazilian Society of Mechanical Sciences and Engineering (2021), pp. 43-67. DOI: 10.1007/s40430-020-02791-8

[16] F. Pérez-Arribas, J. Calderon-Sanchez, A parametric methodology for the preliminary design of SWATH hulls, Ocean Engineering 197 (2020), 106823. DOI: 10.1016/j.oceaneng.2019.106823

[17] B. Yıldız, prediction of residual resistance of a trimaran vessel by using an artificial neural network, Brodogradnja 73 (2022), 1. DOI: 10.21278/brod73107

[18] J. Wang, C. Li, X. Meng, A general calculation method to specify center-of-buoyancy for the stratospheric airship with multiple gas cells, Advances in Space Research 67 (2021), pp. 2517–2533. DOI: 10.1016/j.asr.2021.01.014

[19] S.-I. Moriyama, Y. Watanabe, T. Kurono, J. E. Morais, D. A. Marinho, K. Wakayoshi, Effect of Additional Buoyancy Swimsuits on Performance of Competitive Swimmers, The Open Sports Sciences Journal 14 (2021), pp. 98-105. DOI: 10.2174/1875399X02114010098

[20] J. Wang J, L. Cuichum, X. Meng, A general calculation method to specify center-of-buoyancy for the stratospheric airship with multiple gas cells. Adv Space Res (2021) 67(8), pp. 2517-2533. DOI: 10.1016/j.asr.2021.01.014

[21] R. A. da Paixão, A. M. C. Dutra, E. C. de Oliveira, Modelling, validation, and metrological characterization of tilt densimeters, Measurement 218 (2023), 113122. DOI: 10.1016/j.measurement.2023.113122

[22] M. K. Hirata, R. C. Rigitano, Centro de massa, 2005. Online [Accessed 20 March 2019] [In Portuguese] https://www.ifi.unicamp.br/~lunazzi/F530_F590_F690_F809_F895/F809/F809_sem1_2005/MiguelK-Rigitano_RF.pdf

[23] E. W. Weisstein, Cylindrical Segment, 2010. Online [Accessed 1 April 2019] http://mathworld.wolfram.com/CylindricalSegment.html

[24] JCGM 101. (2008). Evaluation of measurement data — Supplement 1 to the "Guide to the expression of uncertainty in measurement" — Propagation of distributions using a Monte Carlo method, Published by the JCGM in the name of the BIPM, IEC, IFCC, ILAC, ISO, IUPAC, IUPAP, and OIML. Online [Accessed 21 April 2020] https://www.bipm.org/utils/common/documents/jcgm/JCGM_101_2008_E.pdf

[25] X. Wen, Y. Zhao, D. Wang, J. Pan, Adaptive Monte Carlo and GUM methods for the evaluation of measurement uncertainty of cylindricity error. Precision Engineering, 37, (2013), pp. 856–864. DOI: 10.1016/j.precisioneng.2013.05.002